

Manipulator Control with Superquadric Artificial Potential Functions: Theory and Experiments ¹

Richard Volpe ² and Pradeep Khosla ³

The Robotics Institute
Carnegie - Mellon University
Pittsburgh, PA 15213

In **IEEE Transactions on Systems, Man, and Cybernetics**.
Special Issue on Unmanned Vehicles and Intelligent Systems,
20(6), November/December 1990.

¹The material in this paper was partially presented at The IEEE Conference on Robotics and Automation, Philadelphia, PA, 1988

²Department of Physics, Carnegie-Mellon University, Pittsburgh, Pennsylvania, 15213

³Department of Electrical and Computer Engineering, Carnegie-Mellon University, Pittsburgh, Pennsylvania, 15213

List of Figures

1	A repulsive potential added to an attractive well.	5
2	The FIRAS potential.	5
3	The isopotential contours of the FIRAS potential in Figure 2.	6
4	Local minimum creation by the FIRAS potential.	6
5	Superquadric isopotential contours for a rectangle.	9
6	Superquadric isopotential contours for a trapezoid.	9
7	Superquadric isopotential contours for a triangle.	12
8	The superquadric avoidance potential for a rectangle.	12
9	The superquadric avoidance potential for a triangle.	13
10	The superquadric approach potential for a rectangle.	13
11	The superquadric approach potential for a triangle.	18
12	Dynamic superquadric avoidance potential.	18
13	Successful avoidance of an obstacle using the FIRAS potential.	23
14	Unsuccessful avoidance of an obstacle using the FIRAS potential.	23
15	Successful avoidance by a two link manipulator of an obstacle surrounded by a superquadric potential.	23
16	Geometrically limited motion of a two link manipulator avoiding an obstacle surrounded by a superquadric potential.	24
17	Successful avoidance by a three link, redundant manipulator of an obstacle surrounded by a superquadric potential.	24
18	Successfully navigation around four obstacles (a).	25
19	Successfully navigation around four obstacles (b).	25
20	Smooth approach and contact of a rectangle surrounded by a superquadric approach potential.	26
21	Smooth approach and contact of a triangle surrounded by a superquadric approach potential.	26
22	Experimental data from one obstacle avoidance.	28
23	Experimental data from two obstacle avoidance.	28
24	CMU DDARM II control architecture.	32

Abstract

Previous work in artificial potentials has demonstrated the need for an obstacle avoidance potential that closely models the obstacle, yet does not generate local minima in the workspace of the manipulator. This paper presents a potential function based on superquadrics, which closely models a large class of object shapes. This potential function also prevents the creation of local minima when it is added to spherically symmetric attractive wells. We introduce two compatible forms of the superquadric potential function: one for obstacle avoidance, and another for obstacle approach. We have implemented the avoidance and approach potentials in simulations. In these simulations the end effector of the manipulator experiences an attractive force from a global spherical well, while the end effector and each of the links experience repulsive forces from all of the objects. We have also experimentally implemented the avoidance potentials on the CMU DDARM II. The results demonstrate successful obstacle avoidance and approach, and exhibit an improvement over existing potential schemes.

1 Introduction

The problem of moving in space while avoiding collisions with the environment is known as obstacle avoidance or path planning. The obstacle avoidance problem is important for both mobile robots and manipulators [16, 10, 24, 18]. For a mobile robot, the goal is to devise a strategy that will move the robot to its desired destination without colliding with obstacles. In addition, a robust obstacle avoidance scheme should be capable of dealing with moving obstacles. For a manipulator, the problem is more complicated. Not only must the end effector move to the desired destination without collisions with obstacles, but the links of the arm must also avoid collisions. Because this additional requirement is more restrictive, a strategy that works for manipulators can be applied to mobile robots. Therefore, we concern ourselves here with obstacle avoidance for manipulators, and our review of previous work in the field is similarly limited in scope.

Research in the area of obstacle avoidance can be broadly divided into two classes of methodologies: global and local. Global methodologies rely on the description of the obstacles in the configuration space of a manipulator [26, 14, 22]. Local methodologies rely on the description of the obstacles and the manipulator in the cartesian workspace [10, 1, 13].

Global methodologies require that two main problems be addressed. First, the obstacles must be mapped into the configuration space of the manipulator [14]. Second, a path through the configuration space must be found for the point representing the manipulator. Two techniques are used to generate these paths: geometric searches and artificial potentials. The geometric search technique relies on an exhaustive search of the unoccupied configuration space for a continuous path from the start point to the goal point [26, 16, 15, 24, 6]. If a path exists, it will be found. If multiple paths are found, the best may be chosen. The artificial potential technique surrounds the configuration space obstacles with repulsive potential energy functions, and places the goal point at an global energy minimum [21, 22, 19, 29]. The point in configuration space representing the manipulator is acted upon by a force equal to the negative gradient of this potential field, and driven away from obstacles and to the minimum.

Global methodologies have several disadvantages. The algorithms necessary for global methods are computationally intensive. Also, the computational costs increase quickly as a function of the manipulator's degrees-of-freedom: at least exponentially for geometric search techniques, and at least quadratically for potential energy techniques [22]. Thus, they are suited only for off-line path planning and cannot be used for real-time obstacle avoidance. An immediate consequence is that global algorithms are difficult to use for obstacle avoidance in dynamic environments, where the obstacles are moving in time. Also, using global algorithms it is very difficult to describe complicated motion planning tasks such as those arising when two manipulators cooperate.

A viable alternative to global methodologies is provide by local ones [10, 1, 13, 28]. Local methodologies also employ the use of artificial potential functions like those discussed previously. However, unlike configuration space potentials, local potentials are expressed in the cartesian workspace of the manipulator. Obstacles to be avoided are surrounded by repulsive potential functions and the goal point is surrounded by an attractive well. These potentials are added to form a composite potential which imparts forces on a model of the manipulator in cartesian space. Torques equivalent to these forces cause the motion of the

real manipulator.

The main advantage of local techniques is that they are less computationally demanding than global ones. Thus they can be used in real-time control. Further, they provide the necessary framework to deal with dynamic (changing) environments and can be used for real-time obstacle avoidance. Also, when used with a teleoperated manipulator, local artificial potentials provide low level obstacle avoidance. In this case, the path planning of the manipulator is being performed by the operator and the global methodologies lose their value as robust path planners.

However, local methodologies have one distinct problem: the addition of attractive and repulsive potentials can create local minima in the potential function. Any local minimum will cause the manipulator to experience no net artificial force, and thereby stop at an unintended location. A robust artificial potential function model of the environment should have no local minima [12, 27].

In this paper we propose an artificial potential scheme based on the superquadric, a mathematical function which is employed in computer vision and object modelling techniques [2, 3]. This scheme provides obstacle avoidance capability for manipulators in an environment of stationary or moving objects, preventing end effector and link collisions with these objects. This local avoidance scheme provides obstacle avoidance capability without creating local minima.

The superquadric is a deformable parametric surface and is used in our scheme as the isopotential surface for our potential function. Since it is deformable, isopotential surfaces near the object may closely model the object, while surfaces further away can be spherical. These spherical surfaces prevent the formation of local minima when this function is added to a larger spherical attractive potential well.

The assignment of potential energy values to the isopotential surfaces determines the repulsive nature of the function. Two possibilities exist: the avoidance potential function, or the approach potential function. The avoidance potential function has a potential energy value at the surface of the object which is larger than the initial kinetic energy of the manipulator. Thus, an energy barrier is established which cannot be surmounted. The easiest way to ensure that the potential energy barrier is large enough is to force the potential function to go to infinity at the object surface.

We also propose a second type of artificial potential energy function — the approach potential [27, 11]. Instead of having a potential function go to infinity at the object surface (as with the avoidance potential), the potential energy can go smoothly to a finite value less than the kinetic energy of the manipulator. As the manipulator moves toward the object, it gains potential energy, loses kinetic energy, and slows down. But it always has enough kinetic energy to reach the surface. Thus the approach potential provides deceleration forces that ensure a safe contact velocity at the surface. Once stable contact has been established, force control of the manipulator may begin.

This paper is organized as follows: In Section 2 we outline the attributes of artificial potentials by reviewing the work of other researchers. In the course of this review, we indicate those aspects of previous schemes which are valuable, and those aspects which should not be retained. In Section 3 we describe in detail the proposed superquadric potential scheme, and highlight its advantages. In Section 4 we mathematically describe the addition

of the superquadric avoidance potential with global attractive potentials, determine the criterion for the elimination of local minima, and discuss dynamically changing potentials. In Section 5 we evaluate the efficacy of the superquadric potential formulation by simulating both obstacle avoidance and approach. Finally, in Section 6 we present some experimental results of the implementation of the obstacle avoidance potential on the CMU DDARM II.

2 Attributes of Artificial Potentials

The major interest in artificial potential models has been in realizing obstacle avoidance schemes [13, 12, 20, 9, 27]. These schemes require the addition of attractive and repulsive potentials. An attractive potential well is generally a bowl shaped energy well which drives the manipulator to its center if the environment is unobstructed. However, in an obstructed environment, repulsive potential energy hills are added to the attractive potential well at the locations of the obstacles, as in Figure 1. The addition of attractive and repulsive potentials provides obstacle avoidance capability.

In this section, we review the attributes of the attractive and repulsive potential functions that have been proposed. First, we describe the two types of attractive wells: quadratic and conical. Then, we discuss the proposed repulsive potentials and describe the desirable and undesirable properties that each exhibits.

The first type of attractive potential function, the quadratic well, is the most widely used [10, 8, 12]. The reason for this is twofold. First, a quadratic potential well provides a linear control law with constant gain. Consider the quadratic well, U , described by:

$$U(x) = \frac{k}{2} \mathbf{x} \cdot \mathbf{x}, \quad (1)$$

where k is constant and \mathbf{x} is a position vector. The force, \mathbf{F} , from this potential may be obtained by the gradient:

$$\mathbf{F} = -\nabla U = -k\mathbf{x} \quad (2)$$

which is a linear control law (Hooke's Law). Second, all potentials are quadratic for small displacements. This may be seen from the Taylor series expansion in one dimension:

$$U(x_0 + \Delta x) = U(x_0) + \Delta x \left. \frac{dU(x)}{dx} \right|_{x=x_0} + \frac{\Delta x^2}{2} \left. \frac{d^2U(x)}{dx^2} \right|_{x=x_0} + \dots \quad (3)$$

For small displacements, Δx , the higher order terms may be neglected. The force experienced is:

$$F(x_0 + \Delta x) = - \left. \frac{dU(x)}{dx} \right|_{x=x_0} - \Delta x \left. \frac{d^2U(x)}{dx^2} \right|_{x=x_0} - \dots \quad (4)$$

which reduces to Hooke's Law since the first derivative is zero and the second derivative is k . Potentials with positive second derivatives are stabilizing, preventing large displacements from being achieved and keeping the approximation valid. Thus the quadratic well is a good attractive potential because of its simple form and because other potentials reduce to it for small displacements.

A second type of attractive potential function, the conical well, has also been proposed [1]. This function is quadratic within a given range and then increases linearly:

$$U(\mathbf{x}) = \begin{cases} k\mathbf{x} \cdot \mathbf{x}, & |\mathbf{x}| < s \\ 2ks|\mathbf{x}| - ks^2, & |\mathbf{x}| \geq s. \end{cases} \quad (5)$$

The conical well provides a constant magnitude, centrally attractive, force field for distances larger than s . While, for smaller distances, the previously described advantages of the quadratic well are utilized.

The second category of potentials, repulsive potentials, are necessary to repel the manipulator away from obstacles that obstruct its path of motion in the global attractive well. It has generally been recognized that a repulsive potential should have a limited range of influence [1, 10]. This prevents an object from affecting the motion of the manipulator when it is far away from the object. Also, the potential function and its derivative must change smoothly and never become discontinuous [1].

Many proposed repulsive potentials have spherical symmetry. One increases cubically with radial distance inside of a circular threshold range [1]. Another has a Gaussian shape [12]. These potentials are useful for surrounding objects with spherical symmetry and singularities in the workspace. Also, when added to a spherically symmetric attractive well they will not create a local minimum (as will be demonstrated subsequently). But a spherically symmetric repulsive potential does not follow the contour of polyhedral objects. For instance, an oblong object surrounded by a sphere effectively eliminates much more volume from the workspace than is necessary or desirable.

Potentials that follow the object shape were proposed to address the insufficiency of radially symmetric potentials. Examples are the GPF and FIRAS functions [13, 10]. The potential energy, $U(r)$, of the FIRAS function is described by:

$$U(r) = \frac{A}{2} \left(\frac{1}{r} - \frac{1}{r_0} \right)^2 \quad 0 < r < r_0 \quad (6)$$

where r is the closest distance to the object surface, r_0 is the effective range, and A is a scaling factor. Figure 2 shows this potential for $A = 2$ and $r_0 = 6$. The isopotential contours of this potential function are depicted in Figure 3. The GPF function has a similar shape. We shall refer to these as ‘flat-sided’ potentials because of the shape of their isopotential contours.

By itself, a flat-sided potential works well. But when this potential is added to an attractive well, local minima appear on the side of the object away from the center of the well. Consider the case depicted in Figure 4, where the side of the object away from the attractive well center is tangent to the isopotential contours of the well. Motion along the linear section of the object contour, from point A to point B, passes through changing potential values of the attractive well. At points A and B the attractive well potential is higher than at point C. Since the object potential is the same at A, B, and C, the sum of the object potential and the attractive well potential has a local minimum at point C. It can be seen that any section of an object contour that has a radius of curvature greater than the contour of the attractive well will generate a local minimum ‘uphill’ from the object. The contour of a circular repulsive potential always has a smaller radius of curvature than

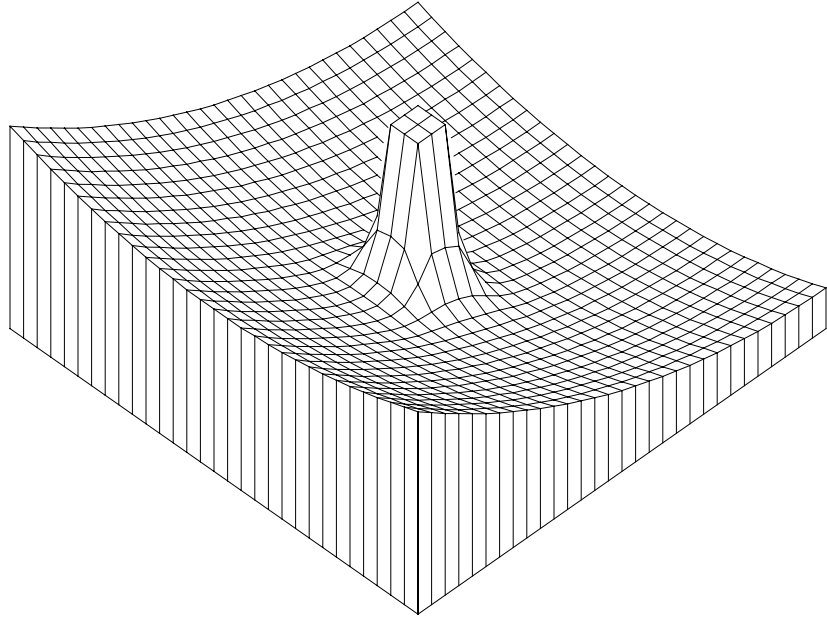


Figure 1: A repulsive potential added to an attractive well.

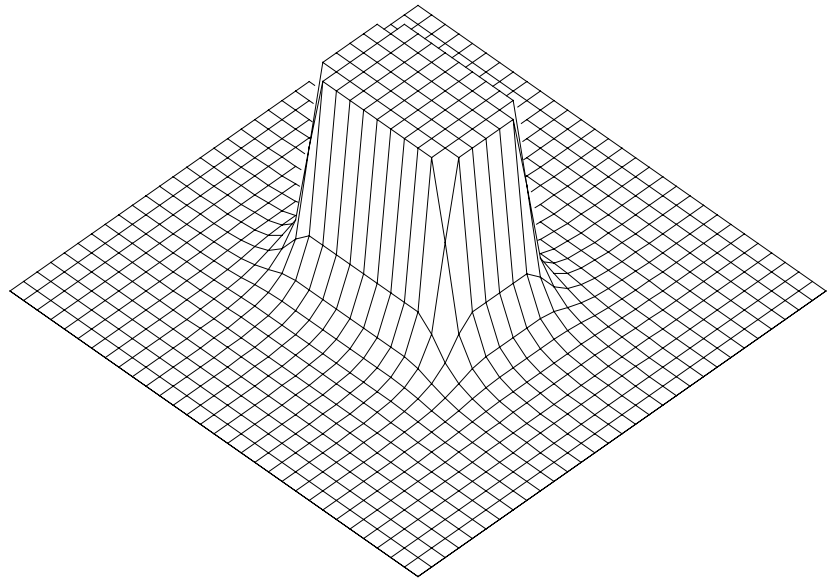


Figure 2: The FIRAS potential for $A = 2$ and $r_0 = 6$. Large values have been truncated.

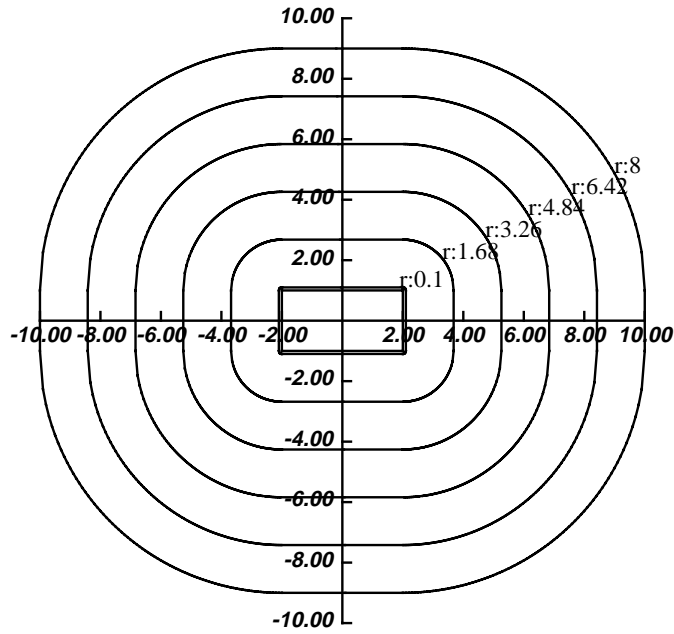


Figure 3: The isopotential contours of the FIRAS potential in Figure 2.

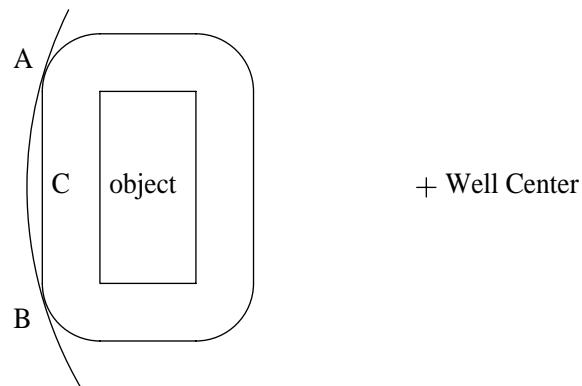


Figure 4: The coincidence of isopotential contours at points A and B indicates the presence of a local minimum in the vicinity of point C.

the contour of the attractive well in which it is inscribed. Therefore, a circular repulsive potential will not generate local minima in this way.

In summary, a repulsive potential function that is useful for modelling objects in the environment should have the following attributes:

1. The potential should have spherical symmetry for large distances to avoid the creation of local minima when this potential is added to an attractive well.
2. The potential contours near the surface should follow the surface contour so that large portions of the workspace are not effectively eliminated.
3. The potential of an obstacle should have a limited range of influence.
4. The potential and the gradient of the potential must be continuous.

We have proposed a novel formulation of a repulsive potential function, based on superquadrics, that satisfies all of the above criteria. Not only is this scheme useful for obstacle avoidance, but it can also be used for obstacle approach. We present this formulation in the next section.

3 Superquadric Potentials

The superquadric potential is a function that has isopotential surfaces shaped like superquadrics. The value of the potential energy at each surface is determined by the potential energy function. We propose two repulsive potential energy functions: the avoidance potential function, and the approach potential function. In this section, we present the superquadric formulation for isopotential contours, and then describe the two types of repulsive potential energy functions.

3.1 Superquadric Isopotential Contours

As is dictated by attributes one and two above, the isopotential contours of a artificial potential function must change from spherical at large distances, to the object shape near the surface.

To obtain isopotential contours that follow the object shape near the surface an object may be surrounded with a superquadric [2, 3]:

$$\left[\left(\frac{x}{f_1(x, y, z)} \right)^{2n} + \left(\frac{y}{f_2(x, y, z)} \right)^{2n} \right]^{\frac{2m}{2n}} + \left(\frac{z}{f_3(x, y, z)} \right)^{2m} = 1 \quad (7)$$

where f_1 , f_2 , and f_3 are scaling functions, and m and n are exponential parameters. Previously we have employed this function in two dimensions ($z = 0$) with constant scaling functions [27]:

$$\left(\frac{x}{a} \right)^{2n} + \left(\frac{y}{b} \right)^{2n} = 1. \quad (8)$$

This form is called an n -ellipse where a is the semi-major axis and b is the semi-minor axis [7, 10]. We first review the use of this simpler form in potential functions and then show how it may be generalized to the superquadric potential form.

In order for the above n -ellipse to be useful as a potential function, two constraints should be imposed at the surface of the object: first, the ellipse must touch the corners of the surrounded object (which is rectangular for this case); and second, the area between the object and the ellipse must be minimal. These constraints yield:

$$a = \frac{w}{2} \left(2^{\frac{1}{2n}}\right) \quad b = \frac{h}{2} \left(2^{\frac{1}{2n}}\right) \quad (9)$$

where w is the x dimension of the rectangle, and h is the y dimension.

At the surface of the object, the isopotential contours should match the shape of the surface. This requires that n go to infinity at the surface. However, away from the surface the contours must become spherical in accordance with the first attribute. Letting n go to one will make the contours elliptical. This ellipse may be further modified by a coefficient that multiplies the y term. The contour function thus becomes:

$$\left(\frac{x}{a}\right)^{2n} + \left(\frac{b}{a}\right)^2 \left(\frac{y}{b}\right)^{2n} = 1 \quad n \geq 1. \quad (10)$$

It is also necessary to have a variable that specifies each contour. The variable acts as a pseudo-distance from the object, being zero at the surface and increasing with successive contours away from the surface. Along the x axis this variable can be made to change linearly. Thus,

$$K = \left[\left(\frac{x}{a}\right)^{2n} + \left(\frac{b}{a}\right)^2 \left(\frac{y}{b}\right)^{2n} \right]^{\frac{1}{2n}} - 1. \quad (11)$$

Figure 5 shows a plot of K at regular intervals with n varying from a very large value to a value near unity.

Since the parameter n must vary from infinity to one while K varies from zero to infinity, n is defined as:

$$n = \frac{1}{1 - e^{-\alpha\beta_n K}} \quad (12)$$

where α and β_n are adjustable parameters. Unless otherwise noted, β_n will be unity. Other definitions of n are possible, but this form is useful because it is related to the magnitude of the potential, as will be shown in Section 3.2.1.

The above description, expanded to three dimensions, yields an ellipsoid instead of an ellipse. For the three dimensional case, f_3 in Equation (7) is a third constant semi-axis, c , and the parameter m can be given the form:

$$m = \frac{1}{1 - e^{-\alpha\beta_m K}}. \quad (13)$$

If the parameter β_m is set equal to β_n , then m equals n and Equation (7) describes an n -ellipsoid.

The elliptical (ellipsoidal) description may be generalized to the superquadric formulation by using nonconstant scaling functions, f_i , in Equation (7). This provides a method of deforming the n -ellipse (ellipsoid) to other shapes. This effect can be interpreted as changing the semi-axes of the ellipse (ellipsoid). We demonstrate this by an example in two dimensions for a superquadric contour that snugly surrounds a trapezoid as shown in

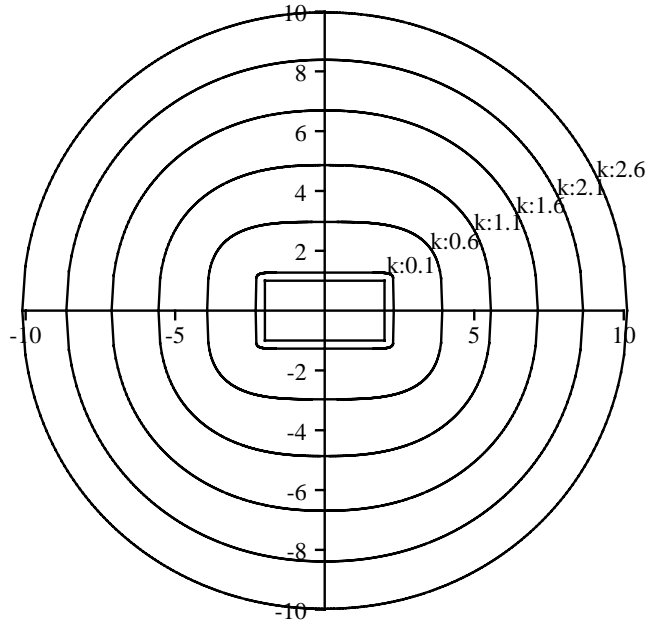


Figure 5: The isopotential contours for $K = 0.1$ to $K = 2.6$, and $\alpha = 1.5$.

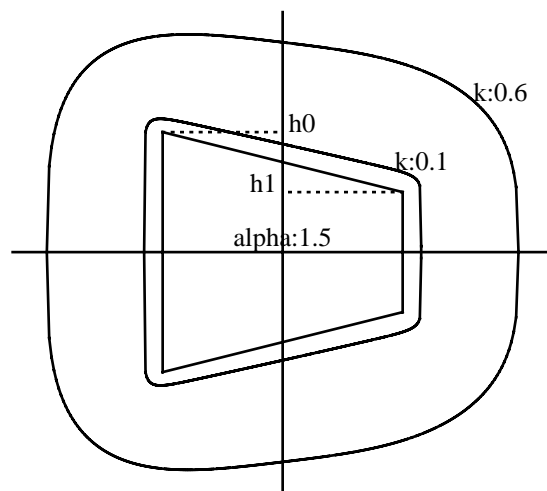


Figure 6: Superquadratic isopotential contours for a trapezoid.

Figure 6. In this case, the semi-minor axis b varies from b_0 to b_1 as the height of the object varies from h_0 to h_1 over its total width, $2w$. Therefore, at the object surface ($K = 0$),

$$b(x) = mx + d \quad (14)$$

$$m = \frac{h_1 - h_0}{2w} = \frac{b_1 - b_0}{2a} \quad (15)$$

$$d = \frac{b_1 + b_0}{2}. \quad (16)$$

This value of b provides a superquadric which touches the corners of the trapezoid, with $K = 0$. Superquadric isopotential contours away from the object are obtained by scaling x :

$$f_2 = m \frac{x}{K + 1} + d. \quad (17)$$

Reducing h_1 to a very small value gives a superquadric model of a triangle, as shown in Figure 7.

Finally, this example can be extended into three dimensions for superquadric models of wedges, pyramids, and cones. For a wedge,

$$f_1 = a \quad (18)$$

$$f_2 = m \frac{x}{K + 1} + d \quad (19)$$

$$f_3 = c. \quad (20)$$

For a pyramid,

$$f_1 = a \quad (21)$$

$$f_2 = m_2 \frac{x}{K + 1} + d_2 \quad (22)$$

$$f_3 = m_3 \frac{x}{K + 1} + d_3. \quad (23)$$

And for a cone oriented along the z -axis,

$$n = 1 \quad (24)$$

$$f_1 = m \frac{z}{K + 1} + d \quad (25)$$

$$f_2 = m \frac{z}{K + 1} + d \quad (26)$$

$$f_3 = c. \quad (27)$$

Thus we have developed a formulation for isopotential contours that are described by superquadrics. With the form of the isopotential contours established, it is necessary to assign potential energy values to them. This is done in the next section.

3.2 Repulsive Potential Energy Functions

The potential energy function must assign potential energy values to the isopotential contours defined previously. We have utilized two types of repulsive energy functions: the avoidance potential, and the approach potential.

3.2.1 The Avoidance Potential

The avoidance potential is a function which surrounds an object and prevents a manipulator from touching the object. This must be true, independent of the manipulator’s kinetic energy. The easiest way to ensure this is to set the magnitude of the potential at the surface to infinity. Away from the surface, the energy values must be in accordance with the third and fourth attributes outlined in Section 2, and in accordance with natural potentials (e.g. electrostatic, gravitational, etc.) exhibit an inverse dependence on distance. Therefore, the potential function must have a K^{-1} dependence for short distance repulsion, but drop to zero faster than K^{-1} for large distances. Also, the function and its derivative must be continuous. A function that has these attributes is the Yukawa potential [5]:

$$U(K) = A \frac{e^{-\alpha K}}{K} \quad (28)$$

Figures 8 and 9 show this function with $\alpha = 1$ and $A = 1$ for a rectangle and a triangle.

The parameter α determines how rapidly the potential rises near the object and falls off away from the object. This rate must be related to the rate at which the ‘ n -ness’ of the ellipse changes as expressed in Equation (12). We have chosen these rates to be proportional, with the constant of proportionality being β_n in Equation (12). Usually, $\beta_n = 1$ and both rates are equal to the value of α .

The parameter A acts as an overall scale factor for the potential. Large values of A will make the object have a spherical field of repulsive force at large distances. Small values of A will allow the object to be approached much more closely. At this closer range, the isopotential contours will have large values of n and will approximate the shape of the object. For the rest of this discussion A will assumed to be unity unless otherwise noted.

3.2.2 The Approach Potential

The approach potential is a function which surrounds an object and decreases the approach speed of the manipulator as it move towards the object. This is achieved by setting the value of the potential energy at the surface of the object to be slightly less than the initial kinetic energy of the manipulator. As the manipulator moves toward the object its kinetic energy is transformed to potential energy, and its velocity decreases. Setting the magnitude of the potential function at the surface less than the initial kinetic energy ensures that the manipulator will always reach the surface.

An appropriate approach potential should have all of the attributes of the avoidance potential, but should go to a finite maximum value at the surface of the object. Therefore, far from the object, the form of the avoidance potential may be used. However, closer to the surface the potential should be Gaussian in nature, the slope smoothly changing to zero at the surface so that no artificial force is experienced when real contact with the environment is established. Because this general form must remain valid for all values of α , a simple polynomial fit is not possible. We propose a function, $U(K)$, which satisfies these criteria:

$$U(K) = \begin{cases} \frac{A}{K} e^{-\alpha K}, & K \geq 1 \\ A \exp\left(-\alpha K^{1+\frac{1}{\alpha}}\right), & 1 > K \geq 0 \end{cases} \quad (29)$$

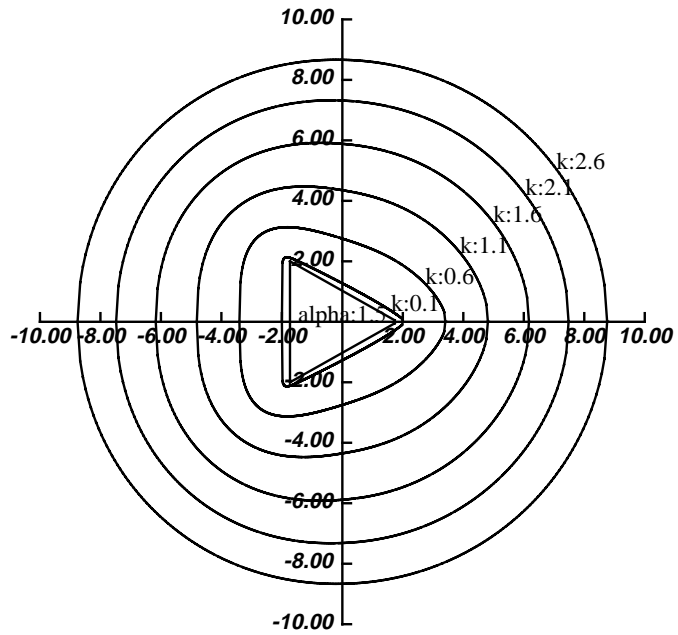


Figure 7: The isopotential contours surrounding a triangle for $K = 0.1$ to $K = 2.6$, and $\alpha = 1.5$.

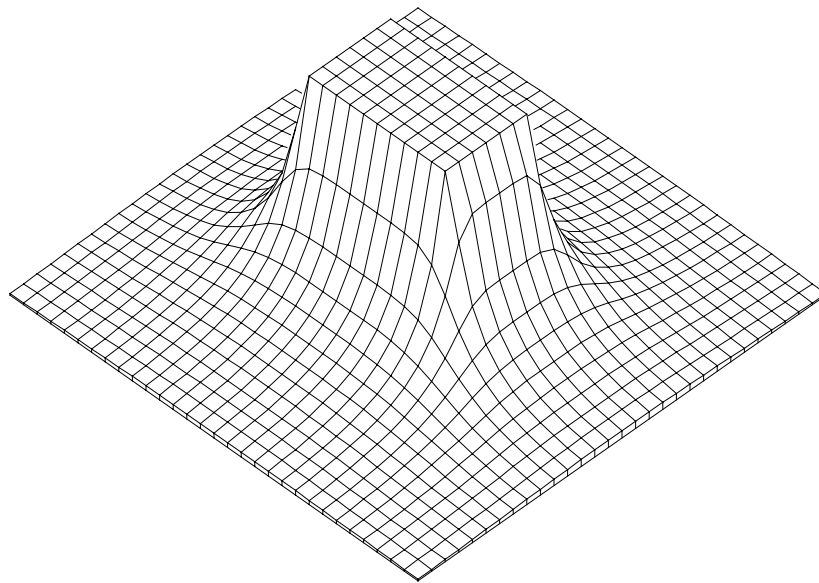


Figure 8: The avoidance potential for a rectangle with $\alpha = 1$ and $A = 1$. Large values have been truncated.

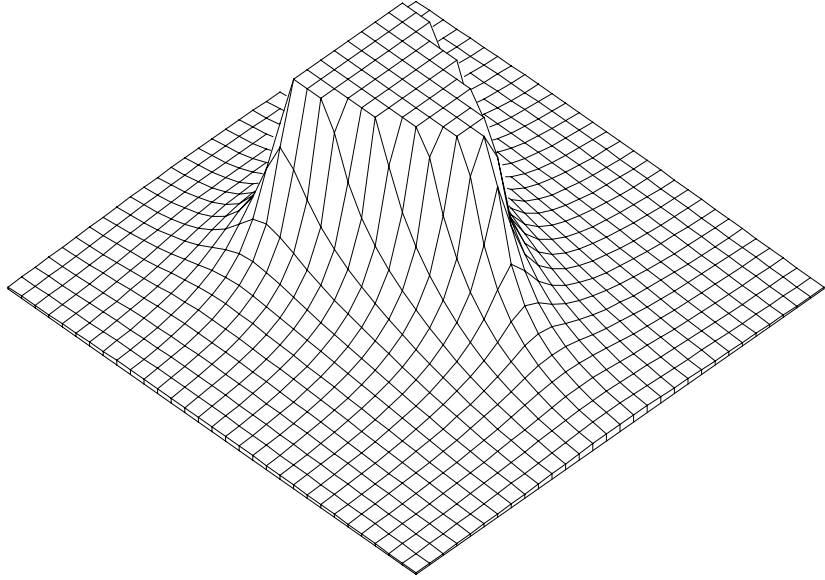


Figure 9: The avoidance potential for a triangle with $\alpha = 1$ and $A = 1$. Large values have been truncated.

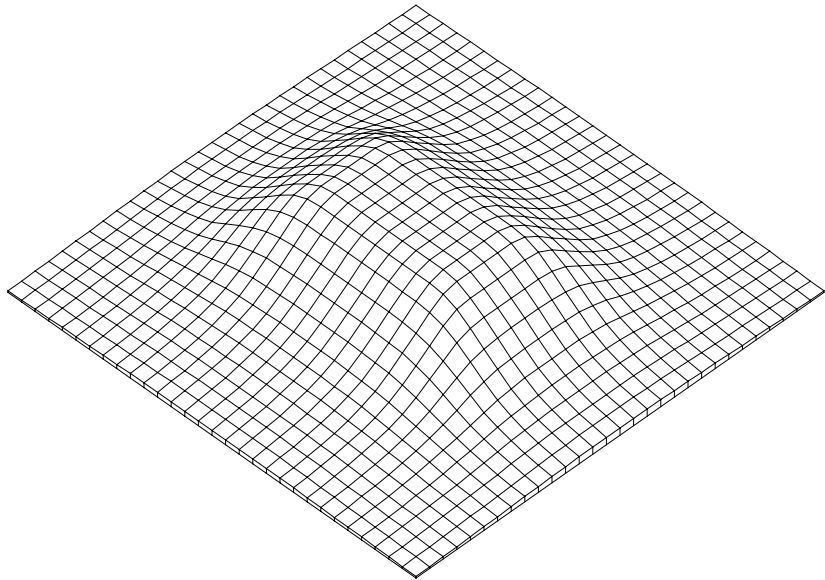


Figure 10: The approach potential function for a rectangle with $\alpha = 1$.

Figures 10 and 11 show this function with $\alpha = 1$ for a rectangle and a triangle.

In this section, we have presented a superquadric isopotential contour formulation and the two types of repulsive potential energy functions. The developed superquadric potentials have the attributes outlined in Section 2, but only asymptotically. The major concern raised by this fact is the avoidance potential is never exactly circular (because K is never infinite in practice). Thus, attribute number one may be violated when the avoidance potential is added to a spherical attractive well. This issue is explored analytically in the next section.

4 Addition of Superquadric Avoidance Potentials and an Attractive Well

When adding superquadric avoidance potentials to a global attractive well, several situations must be considered. These may be divided into single object and multi-object scenarios.

For a single obstacle (only one avoidance potential), the relation between the positions of the avoidance potential and the global well center is important. Three distinct situations arise. First, the global well center is far from the object and is not effected by the object potential. Second, the global well center is inside the object to be avoided. Or third, the situation which is between the above two extremes, the global well center is within the range of influence of the avoidance potential. The second case will not be considered any further since it precludes the possibility of having the manipulator obtain the goal position. The remaining two situations, will be discussed in Sections 4.1 and 4.2.

If multiple objects are to be added to a global attractive well, the relation of these objects to each other is of primary importance. (The effect of the position of each to the global well center is covered by the single object analysis.) If multiple objects are placed at distances from each other such that the addition of their potential energy is nonzero, then the single object analysis breaks down. For example, multiple objects may be placed in a cluster a such a way that they effectively form a larger object with a concavity that faces away from the global well center. This concavity may cause a local minimum that can trap the manipulator. To avoid this problem, the object cluster and its concave regions may be treated as one large object and surrounded with one potential. However, this solution will obviously not work as the workspace become heavily populated with obstacles. We believe that in this case a higher level trajectory planner will become necessary, and we do not address the scenario any further. Therefore, the following analysis is restricted to a single obstacle in a global well.

4.1 Addition of A Superquadric Avoidance Potential to a Distant Attractive Well

The concern when adding an avoidance potential to a distant attractive well, is that an undesirable minimum may be created ‘uphill’ from the object. Because the superquadric avoidance potential only becomes a circle asymptotically, a spurious minimum may be present. However, this minimum can effectively be removed by making the depression associated with it smaller than the resolution of the system.

For a rectangular object, the minimum value of α is determined for its worst case orientation. This is when the longest dimension of the object is normal to the shortest distance between the starting position and the attractive well center. In other words, the object is placed ‘across’ the desired path. In this configuration, the isopotential contours of the object to be avoided are tangent to the isopotential contours of the attractive well. Using a coordinate system centered on the object, and the x -axis along its longest dimension, the isopotential contours have a slope of zero and an infinite radius of curvature along the y -axis. This can be seen by rearranging Equation (11) as $y = f(x)$, taking the first and second derivatives, and setting $x = 0$. Mathematically, the superquadric is linear at the axes when $n \neq 1$. Thus, *mathematically* we have the same problem that was described earlier — an isopotential object contour with a radius of curvature larger than the spherical well in which it is placed will definitely cause minima if it is placed tangent to the well. However, this problem can be effectively eliminated for the superquadric potential function by adjusting the parameter alpha. The adjustment makes the depression from local minimum smaller than the resolution of the system. This solution is presented in detail below.

Consider again a coordinate system centered on the object, oriented as described above. The potential energy, U , has the following form:

$$U = U_o(K) + U_w(\mathbf{x}) \quad (30)$$

where the object and well potentials are obtained from Equations (28) and (1) as:

$$U_o = \frac{e^{-\alpha K}}{K} \quad \text{and} \quad U_w = \ell \mathbf{x} \cdot \mathbf{x} \quad (31)$$

with ℓ constant and $\mathbf{x} = (x, y - y_0)$, where y_0 is the location of the attractive well center.

First it is necessary to find the local minimum along the y -axis that is on the opposite side of the object from the attractive well center. At this point the total force is zero.

$$0 = \nabla U = \frac{\partial}{\partial x} [U_o + U_w] \hat{x} + \frac{\partial}{\partial y} [U_o + U_w] \hat{y} \quad (32)$$

or

$$0 = \frac{\partial U}{\partial K} \left[\left(\frac{x}{a} \right)^{2n} + \left(\frac{b}{a} \right)^2 \left(\frac{y}{b} \right)^{2n} \right]^{\frac{1}{2n}-1} \left(\frac{1}{a} \right)^{2n} x^{2n-1} + 2\ell x \quad (33)$$

$$0 = \frac{\partial U}{\partial K} \left[\left(\frac{x}{a} \right)^{2n} + \left(\frac{b}{a} \right)^2 \left(\frac{y}{b} \right)^{2n} \right]^{\frac{1}{2n}-1} \left(\frac{b}{a} \right)^2 \left(\frac{1}{b} \right)^{2n} y^{2n-1} + 2\ell(y - y_0) \quad (34)$$

where

$$\frac{\partial U}{\partial K} = -e^{-\alpha K} \left[\frac{\alpha}{K} + \frac{1}{K^2} \right]. \quad (35)$$

Considering only the y direction at the y -axis ($x = 0$),

$$\frac{\partial U}{\partial y} \Big|_{x=0} = \frac{\partial U}{\partial K} \left[\left(\frac{b}{a} \right)^2 \left(\frac{y}{b} \right)^{2n} \right]^{\frac{1}{2n}-1} \left(\frac{b}{a} \right)^2 \left(\frac{1}{b} \right)^{2n} y^{2n-1} + 2\ell(y - y_0) \quad (36)$$

is a cubic equation of the form:

$$0 = -e^{-\sigma}(\sigma + 1)c + 2\ell(y - y_0)(cy - 1)^2 \quad (37)$$

with

$$K(x=0) = cy - 1, \quad c \equiv \left(\frac{b}{a}\right)^{\frac{1}{n}} \left(\frac{1}{b}\right), \quad \sigma \equiv \alpha K. \quad (38)$$

Solving for the one real root of this equation yields:

$$y = \frac{1}{c} \left(M + N + \frac{1}{3}(2 + cy_0) \right) \quad (39)$$

where

$$M = \left[-\frac{h}{2} + \sqrt{\frac{h^2}{4} + \frac{g^3}{27}} \right]^{\frac{1}{3}} \quad N = - \left[\frac{h}{2} + \sqrt{\frac{h^2}{4} + \frac{g^3}{27}} \right]^{\frac{1}{3}} \quad (40)$$

$$g = -\frac{1}{3}(y_0 - 1)^2 \quad (41)$$

$$h = \frac{1}{27} \left[2 - 6y_0 - 6y_0^2 - 2y_0^3 - 27c \left(\frac{\sigma + 1}{2\ell} \right) e^{-\sigma} \right]. \quad (42)$$

Having solved for the y coordinate of the minimum, it is necessary to determine the size of the local depression. This is done by finding the first maximum in the x direction for the y value obtained. The value of x is obtained from Equations (33) and (34) as:

$$x = \frac{a}{b} \left[\frac{y^{2n-1}}{y - y_0} \right]^{\frac{1}{2n-2}}. \quad (43)$$

Given that the resolution of the system being modelled must be less than $2x$, it is only necessary to satisfy the above equation. Because y and n are both functions of σ , this equation can be used for an iterative solution of σ . With a value of σ determined, y and n may be obtained from Equations (12), (37), and (38). Then K and α may be obtained from Equations (38). In this way, a minimum value of α may be calculated which permits the addition of attractive and repulsive potentials without the creation of a local minimum.

For a rectangular object in the conical well, a similar analysis may be performed. In this case U_w in Equation (30) is obtained from Equation (2) as:

$$U_w = 2\ell s|\mathbf{x}| - \ell s^2. \quad (44)$$

Therefore, Equation (32) yields:

$$0 = \frac{\partial U}{\partial K} \left[\left(\frac{x}{a}\right)^{2n} + \left(\frac{b}{a}\right)^2 \left(\frac{y}{b}\right)^{2n} \right]^{\frac{1}{2n}-1} \left(\frac{1}{a}\right)^{2n} x^{2n-1} + \frac{2\ell s x}{|\mathbf{x}|} \quad (45)$$

$$0 = \frac{\partial U}{\partial K} \left[\left(\frac{x}{a}\right)^{2n} + \left(\frac{b}{a}\right)^2 \left(\frac{y}{b}\right)^{2n} \right]^{\frac{1}{2n}-1} \frac{b^{2-2n}}{a^2} y^{2n-1} + \frac{2\ell s(y - y_0)}{|\mathbf{x}|}. \quad (46)$$

Again, considering only the y direction at the y -axis,

$$\left. \frac{\partial U}{\partial y} \right|_{x=0} = \frac{\partial U}{\partial K} \left[\left(\frac{b}{a} \right)^2 \left(\frac{y}{b} \right)^{2n} \right]^{\frac{1}{2n}-1} \left(\frac{b}{a} \right)^2 \left(\frac{1}{b} \right)^{2n} y^{2n-1} + 2\ell s \quad (47)$$

is a quadratic equation of the form:

$$0 = -e^{-\sigma}(\sigma + 1)c + 2\ell s(cy - 1)^2. \quad (48)$$

Solving for the meaningful root of this equation yields:

$$y = \frac{1}{c} + \sqrt{\frac{e^{-\sigma}(\sigma + 1)}{2\ell s c}}. \quad (49)$$

As before, the y coordinate of the minimum is used to determine the size of the local depression. This is done by finding the first maximum in the x direction for the y value obtained. The value of x is obtained from Equations (45) and (46), and is equivalent to Equation (43). As was outlined before, a solution for α may then be obtained.

For non-rectangular objects in quadratic and conical wells, the same analyses may be used as worst case scenarios. The rectangle considered will have the dimensions of the maximum height and width of the non-rectangular object. A valid bound for α is determined since the rectangle is more likely to form a local minima. As was described previously, this is because the superquadric isopotential contours that intersect the object axes at right angles have an infinite radius of curvature at the points of intersection. The parameter α eliminates the local minimum by forcing the depression associated with it to become smaller than the resolution of the system. This is equivalent to saying that the parameter α forces the isopotential contours to circles (within the resolution of the system) at the range of the former minimum. For a non-rectangular object the same value of α will also provide circular isopotential contours at the necessary range, ensuring that these objects will not cause local minima.

4.2 Addition of a Superquadric Avoidance Potential to a Close Attractive Well: Dynamic Potentials

The previous analysis determines a value of the parameter α that prevents the formation of a local minimum ‘uphill’ from the obstacle. However, it is assumed that independent of the value of α , the object potential will be zero at the center of the global attractive well. If this is not the case, the addition of the global well and the object potential will displace the global minimum from the center of the global well. In Figure 12(a) the global minimum will move from point C to point D. This implies that the manipulator will not achieve the goal point even though no local minima are present in the environment. Increasing α may eliminate this problem by reducing the range of the object potential. However, if the global well center is within the smallest sphere (circle) that can enclose the object, then increasing α will not help. Since there is no way for the isopotential contours to become circular inside this range, the value of the object’s avoidance potential can not go to zero, by design. If the parameters A or β_n are modified to force the obstacle potential to zero at the global well center, they will also cause the obstacle potential to become nonspherical,

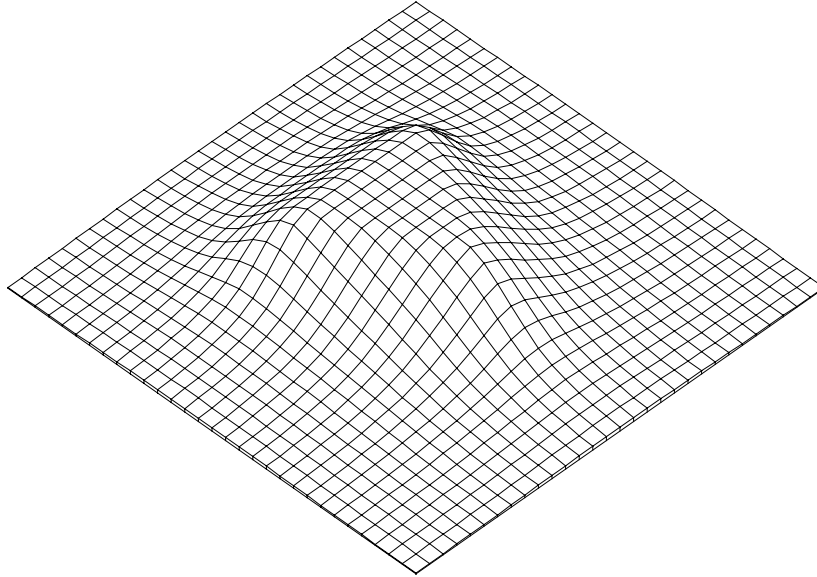


Figure 11: The approach potential function for a triangle with $\alpha = 1$.

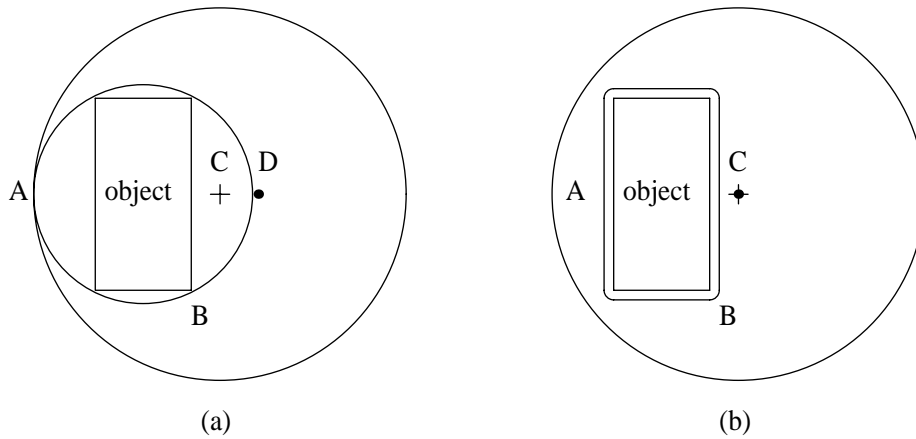


Figure 12: These figures show the effect of having the global well center, point C, very close to an obstacle. In (a) the elimination of a local minimum at point A moves the global minimum from C to D. In (b), reshaping the object potential moves the global minimum to the global well center, point C. This causes the formation of a local minimum at point A. However, if the manipulator has already moved to point B before the potential changes shape, the new local minimum will provide no problem.

as in Figure 12(b). This nonspherical shape will cause the formation of a local minimum on the other side of the obstacle at point A, as discussed in Section 2.

Thus a dilemma exists: to avoid the creation of a local minimum, the position of the global minimum must be shifted; and to remove this shift, a local minimum must be created. The only solution to this problem is to dynamically change the potential shape. Thus, if the manipulator is ‘uphill’ from the object, the parameters must be set to eliminate the formation of the local minimum. As the manipulator moves to the ‘downhill’ side of the obstacle, near point B in Figures 12(a) and 12(b), the potential parameters may be changed to shrink the object potential. This will move the global minimum back to the center of the global attractive well at point C in Figure 12(b). There will then be the formation of a local minimum ‘uphill’ from the object at point A in Figure 12(b), but this is of no concern since that region of the workspace has already been traversed.

This process of dynamically altering the shape of the avoidance potential is not possible with the potentials that have been previously reviewed, and is presented here as another advantage intrinsic to the superquadric potential formulation.

5 Simulation

To test these concepts the performance of two link and three link (redundant) planar manipulators interacting with an artificial potential have been simulated. The motion of these arms is caused by the artificial forces acting on the end effector and the individual links. The end effector is attracted by a goal point and repelled by the obstacle, while the links are repelled by the obstacle if the link interaction is ‘on’. Our results indicate that the superquadric potentials provide a valid method of obstacle avoidance for a manipulator, and an improvement over existing potential functions.

5.1 End Effector Interaction

There are two ways for the arm to react to the artificial forces applied to the end effector. The first method transforms the forces into the corresponding joint torques through the transpose of the Jacobian: $\tau = J^T F$. The joint accelerations can then be derived from the Lagrangian [4]. The second method obtains joint accelerations by directly transforming the Cartesian accelerations that would be experienced by a unit mass in the potential well: $\ddot{\theta} = J^{-1} (\ddot{x} - \dot{J}\dot{\theta})$. The first method is desirable because it does not involve the inverse of the Jacobian, which may become singular. For avoidance potentials, the first method is used. But the second method must be used when employing an approach potential.

The approach potential concept requires that the final potential energy of the manipulator be less than or equal to the initial sum of the kinetic and potential energy. Thus, as the arm approaches the object, all of its kinetic energy is converted to potential energy and the arm stops at the surface. While the kinetic energy of the arm may be obtained from the Lagrangian, the artificial potential energy of the arm cannot [4]. (In fact, the potential energy in the Lagrangian is zero because the manipulator used in these simulations is assumed to be operating in a plane perpendicular to the force of gravity.) Instead, the potential energy must be obtained from the position of the manipulator links in the potential well. Even for a two link arm with one dimensional links and uniform density, λ , this potential energy has

the form:

$$\begin{aligned}
PE = & \int_{K(\text{base})}^{K(\text{elbow})} A\lambda \frac{e^{-\alpha K}}{K} dK + \int_{K(\text{elbow})}^{K=1} A\lambda \frac{e^{-\alpha K}}{K} dK \\
& + \int_{K=1}^{K(\text{end effector})} A\lambda \exp\left(-\alpha K^{1+\frac{1}{\alpha}}\right) dK + PE(\text{potentialwell}) \quad (50)
\end{aligned}$$

assuming that the end effector is at a distance of $K \leq 1$ away from the object. Obviously, this form of the potential energy is intractable. Hence it is not used in the Lagrangian and can not be used in this approach potential scheme.

Instead, the kinetic and potential energy is obtained from the motion of a unit point mass located at the end of the arm. Therefore, the second method of end effector interaction must be used to determine this motion.

5.2 Link Interaction

While there are two methods for determining the end effector interaction that will guide it around obstacles, neither method alone will prevent collisions of the links with the obstacles. To prevent these collisions, there must be an interaction of the links with the the artificial force field. But a link occupies a region near the obstacles, not just a point. How then should the interaction be calculated? It would be too costly to integrate the total interaction of the link with the field. Also, it is the avoidance of collision that is of primary importance. Therefore, the point on the link which is closest to the obstacle should determine the amount of repulsion experienced. The following is an algorithm which determines the point on a link which is closest to an obstacle.

1. Consider the obstacle corner points with respect to the link sides.
 - (a) Consider the line determined by two successive corners of the link. This line defines two half planes, one of which doesn't contain the link.
 - (b) If all four of the obstacle corner points are in the halfplane without the link, proceed. Consider only the point which is closest to the halfplane edge.
 - (c) Project this obstacle corner point onto the halfplane edge.
 - i. If the perpendicular projection is within the side of the link then the obstacle–corner–point / link–side distance is returned as well as the point of projection on the link side.
 - ii. Otherwise, the distance from the obstacle corner point to the closer corner of the link side is saved, as well as this link corner's coordinates.
 - (d) After considering all four link sides, save the closest distance obtained and the corresponding link corner point.
2. Consider the link corner points with respect to the obstacle sides. Repeat steps 1.a through 1.d, interchanging the roles of the link and obstacle.

3. If steps 1.c.i or 2.c.i have not caused a return, determine the closer of the distances saved in steps 1.d and 2.d, and return this value with the corresponding link corner point.

Once the closest point of the link to the object has been determined, the artificial force is calculated. This force vector and the closest point determine the line of force. The line segment which runs through the axis of rotation of the link, along its length, acts as the leverarm. The point of intersection of the line of force with the line that contains the leverarm determines the length of the leverarm. If the leverarm is longer than the link length then it is set to the link length. If the leverarm is less than zero (that is, it extends from the axis in the direction opposite of the link) then it is set to zero. The length of this leverarm for link N is denoted a_N .

The torque exerted on the joints is determined by a Jacobian for each link. Thus, for force on the N th link the torque is $\tau_N = J_N^T F_N$, where the transposes of the Jacobians for a three link manipulator are:

$$J_1^T = \begin{bmatrix} 0 & a_1 C_1 \\ -a_1 S_1 & 0 \\ 0 & 0 \end{bmatrix} \quad (51)$$

$$J_2^T = \begin{bmatrix} -l_1 S_1 - a_2 S_{12} & l_1 C_1 - a_2 C_{12} \\ -a_2 S_{12} & a_2 C_{12} \\ 0 & 0 \end{bmatrix} \quad (52)$$

$$J_3^T = \begin{bmatrix} -l_1 S_1 - l_2 S_{12} - a_3 S_{123} & l_1 C_1 - l_2 C_{12} + a_3 C_{123} \\ -l_2 S_{12} - a_3 S_{123} & a_2 C_{12} + a_3 C_{123} \\ -a_3 S_{123} & a_3 C_{123} \end{bmatrix} \quad (53)$$

where S and C denote sine and cosine, and the subscripts indicate their arguments which are the sum of the corresponding angles. For a two link manipulator, J_1^T and J_2^T may be used, ignoring the third row.

The total torque caused by the interaction of the links with the repulsive field of the obstacle is simply: $\tau = \sum \tau_N$.

5.3 Simulation Experiments

Three main situations were examined: 1.) Motion to a goal point while avoiding an object surrounded by a flat-sided potential, 2.) Movement to a goal point while avoiding an object surrounded by the proposed superquadric avoidance potential, 3.) and approach of an object surrounded by the proposed superquadric approach potential. In the first two situations the end effector experiences an attractive force from a goal point and a repulsive force from the obstacle, and the links of the arm experience a repulsive force from the obstacle. For the third situation, the use of a goal point is optional and there is no link interaction.

5.3.1 Flat-Sided Potential

Figure 13 shows the simulated manipulator moving from the initial position to the goal position, successfully avoiding the obstacle. In this simulation the FIRAS potential was

used as the avoidance potential around the obstacle. For this initial configuration of the manipulator the FIRAS potential works well. However, the repulsive force experienced by the links substantially aids the end effector’s motion around the obstacle. To minimize this help, the end effector can be made to approach the obstacle while normal to its surface. This configuration, shown in Figure 14 accentuates the effect of the local minimum on the “uphill” side of the obstacle. With the link interaction reduced, the end effector settles into this local depression in the potential and stops.

5.3.2 Superquadric Avoidance Potential

The same arm trajectories have been initiated with the superquadric potential in the circular attractive well. Figures 15 and 16 show the end effector of a two link manipulator successfully navigating around the obstacle. This confirms the absence of a local minimum ‘uphill’ from the object. However, with only two degrees of freedom, the arm can not move completely around the obstacle when configured as in the second example — it becomes stuck when the repulsive torque of the obstacle on the second link equals the attractive torque of the goal point on the end effector. This is not a deficiency in the form of the potential, but a deficiency in the two link manipulator. Figure 17 shows that a three link design does not have this same problem. The arm is able to ‘snake’ around the obstacle, and the end effector is able to achieve the goal point.

A third situation was also examined. Four obstacles surrounded by superquadric avoidance potentials were placed in a conical attractive well. Figures 18 and 19 show the manipulator successfully navigating between them to achieve the specified goal point. The start and finish points were interchanged for the two simulations. Different trajectories were created, but the traversal time was about the same.

5.3.3 Approach Potential

Finally, the motion of the end effector approaching the surface of a rectangle and a triangle has been simulated in Figures 20 and 21. For these simulations, no attractive point was used. Instead, the arm was given an initial end effector velocity with its corresponding kinetic energy. The height of the potential at the surface was set to ninety percent of the initial kinetic and potential energy. To eliminate any computational errors due to the discrete time nature of the calculations, the height of the potential was continually modified to ninety percent of the kinetic and potential energy. Also, the end effector was position controlled in the direction parallel to the surface.

6 Experiments

We have implemented the proposed avoidance strategy as a controller on the CMU DDARM II system. The current implementation prevents collisions of the end effector with obstacles in a two dimensional horizontal plane. Since the CMU DDARM II is a SCARA configuration arm the end effector hangs down into the plane, eliminating the need for the calculation of link interaction forces.

Figure 22 shows multiple paths taken by the end effector in successive experiments from

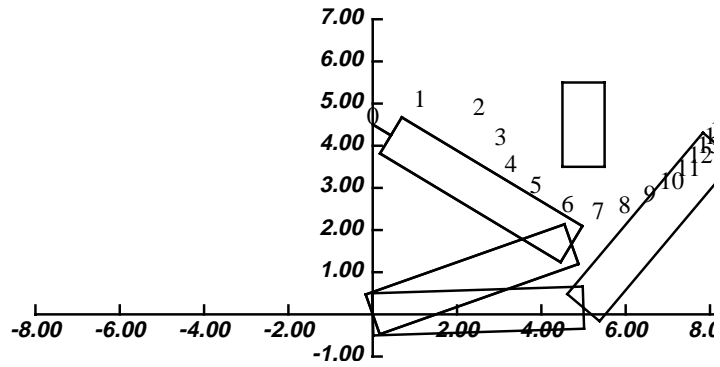


Figure 13: Successful avoidance of an obstacle using the FIRAS potential ($r_0 = 1.5$).

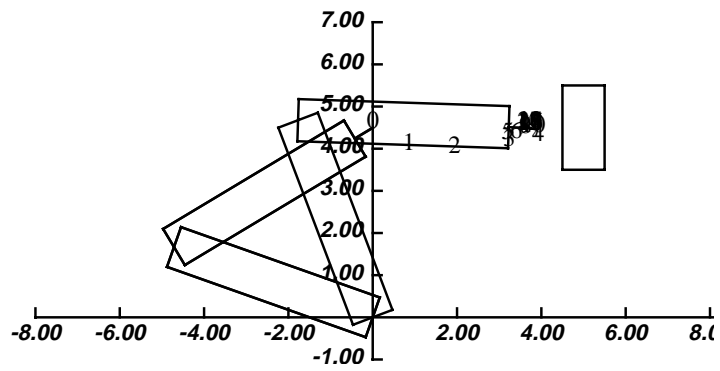


Figure 14: Unsuccessful avoidance of an obstacle using the FIRAS potential ($r_0 = 1.5$). The end effector has settled in a local minimum just ‘uphill’ from the obstacle.

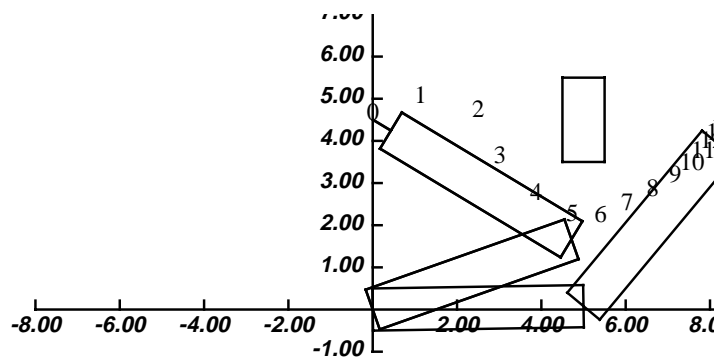


Figure 15: Successful avoidance of an obstacle using a superquadratic potential ($\alpha = 7.0$).

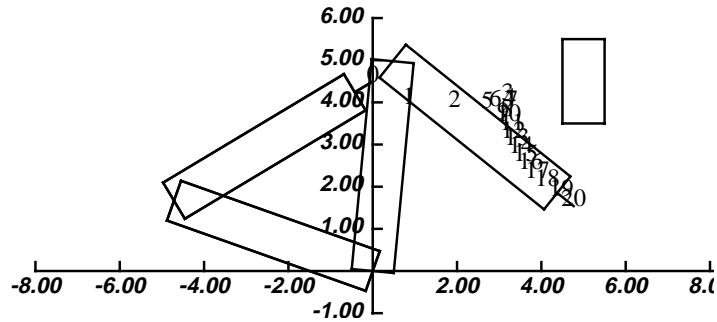


Figure 16: Successful avoidance of an obstacle using a superquadric potential. The minimum value of α that will allow avoidance has been used ($\alpha = 4.4$). The arm is prevented from reaching the goal by its geometric limitations.

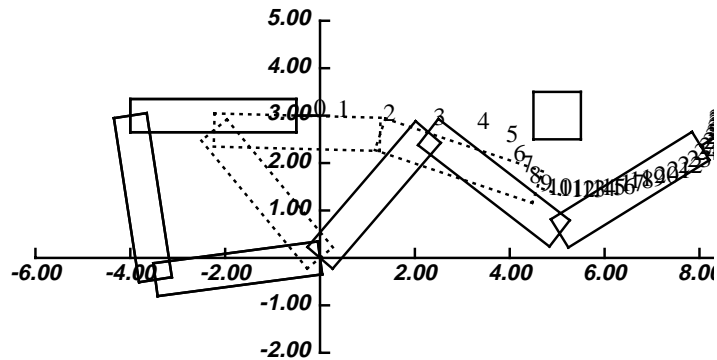


Figure 17: Successful avoidance of an obstacle using the newly proposed function. The minimum value of α that will allow avoidance has been used ($\alpha = 3.76$). The redundancy of the manipulator enables it to 'snake' its way around the obstacle. The dotted manipulator is an intermediate configuration.

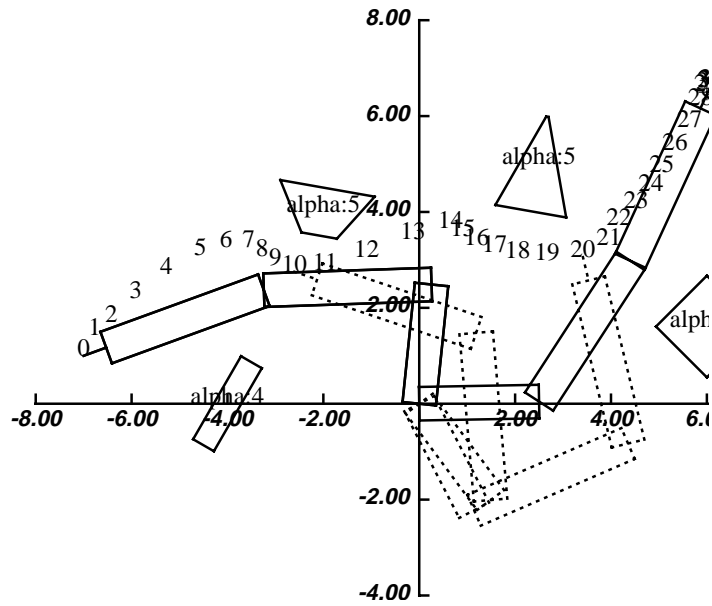


Figure 18: Successful navigation around four obstacles using superquadric avoidance potentials and a modified conical attractive well. The dotted manipulators are intermediate configurations.

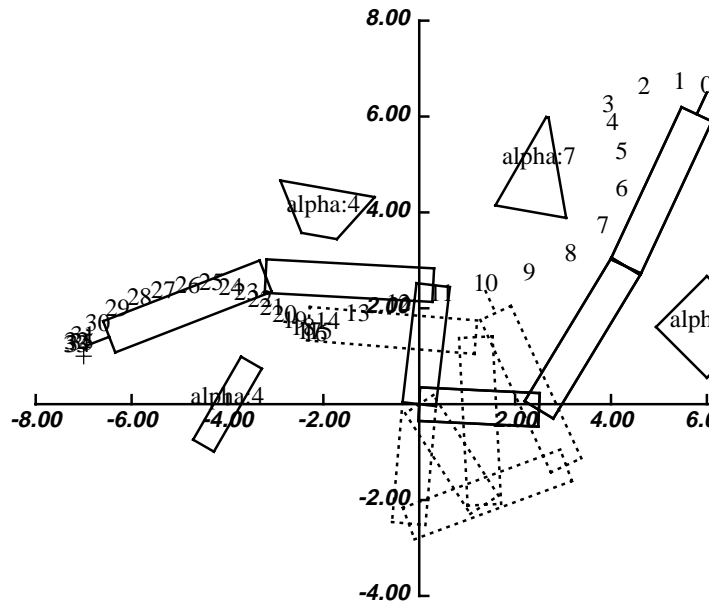


Figure 19: The same situation as Figure 18 except that the starting and ending points have been interchanged. Notice that a different trajectory has been created but the time of traversal is about the same.

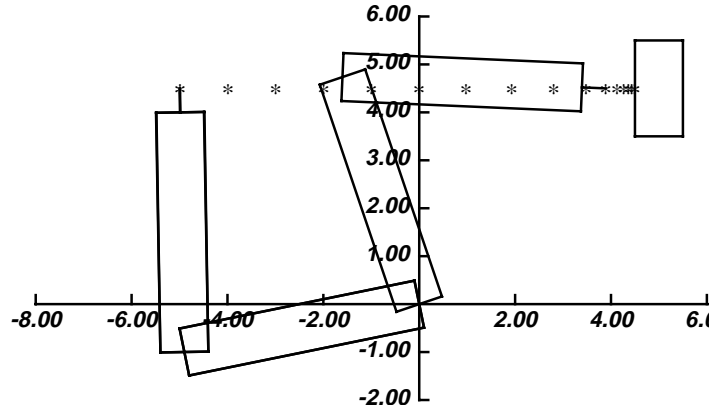


Figure 20: This figure shows successful approach and contact with a rectangle surrounded by the proposed approach potential. For this simulation there was no attractive point, but the end effector was position controlled in the y direction. The initial velocity was 1 unit/sec in the x direction. The contact velocity was 0.06 unit/sec.

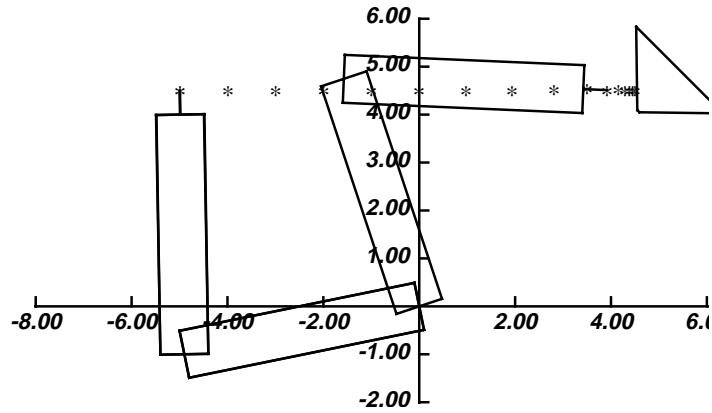


Figure 21: This Figure shows successful approach and contact with a triangle surrounded by the proposed approach potential. For this simulation there was no attractive point, but the end effector was position controlled in the y direction. The initial velocity was 1 unit/sec in the x direction. The contact velocity was 0.05 unit/sec.

different starting positions in a conical well. The end effector always reaches the goal point even though different directions may be taken around the obstacle. Notice that no local minimum is encountered.

Figure 23 shows a path taken to successfully navigate between two obstacles in a conical well. The potential around the rectangle, as evidenced by the path taken, is essentially spherical. This is necessary to prevent the creation of a local minimum in front of it. The path around the triangle, however, follows its shape more closely. This was accomplished by reducing the parameter A . No minimum is created due to the triangle's orientation.

The superquadric avoidance potentials have also been used while the manipulator is under control of a joystick. In this scenario the operator is prevented from inadvertently driving the manipulator into the obstacles by the repulsive force of the avoidance potentials. The obstacle potentials are given a small range (by reducing A) so that very little of the workspace is eliminated. No global well is used. Effectively, this scenario replaces the artificial potential path generation with the much higher level path planning of the operator. However, the superquadric avoidance potentials still remain valuable as a preventative measure against operator error.

The current implementation calculates the artificial forces due to the global well potential and the superquadric object potential. Commanded joint torques may be calculated by use of the transpose of the Jacobian or by using resolved acceleration control [17]. The algorithm runs at a peak speed of 375 Hz for one object, 200 Hz for two objects. Due to the sequential computation of the object potentials, addition of other obstacles to the environment increases the computational requirements linearly. Parallelization of the code could be easily implemented with the addition of more processors, yielding a control rate equal to that for one object. Object positions are currently constant valued variables in the control code, but visual feedback will in the future provide object position data in real time, enabling dynamic obstacle avoidance.

The newly developed control system for the CMU DDARM II is pictured in Figure 24. The real-time controller runs on an Ironics 68020 under Chimera, a real-time kernel for the Ironics [23, 25]. The real-time control processor is separated from the Unix environment of its Sun 3/260 host by a VME to VME bus repeater. All control computation is done on a Mercury MC3200 floating point processor at a rate of approximately 7 Mflops. Communication with the DDARM is performed through six Texas Instruments TMS320 processors (one for each joint).

7 Summary

A novel superquadric potential has been developed that provides obstacle avoidance and object approach capabilities. Robust obstacle avoidance and goal acquisition is achieved by governing the end effector motion with an avoidance potential placed in an global attractive well. Local minima are not generated in the workspace because of the asymptotically spherical nature of the superquadric potential. Link collisions with the environment are also eliminated by our scheme. For object approach, a second form of the superquadric potential may be employed to generate deceleration forces. This scheme reduces contact velocities and forces to tolerable levels. Both the avoidance and approach potentials have been implemented in simulations of two and three link manipulators. The avoidance poten-

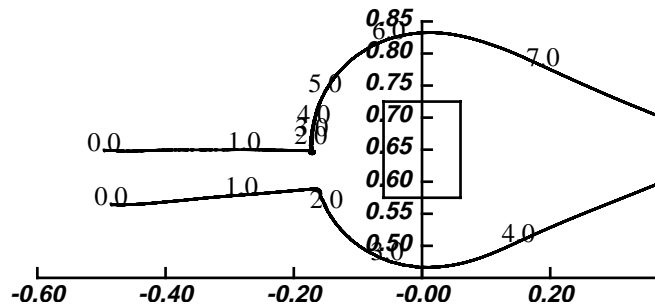


Figure 22: Experimental data showing two paths taken to successfully avoid an obstacle by using the superquadratic avoidance potential in a conical well. The well parameters are: $k = 150$ N/m, $s = 0.1$ m, damping = 150 N · s/m. The object potential parameters are: $\alpha = 20$, $A = 0.1$. The numbers along the paths indicate the time in seconds.

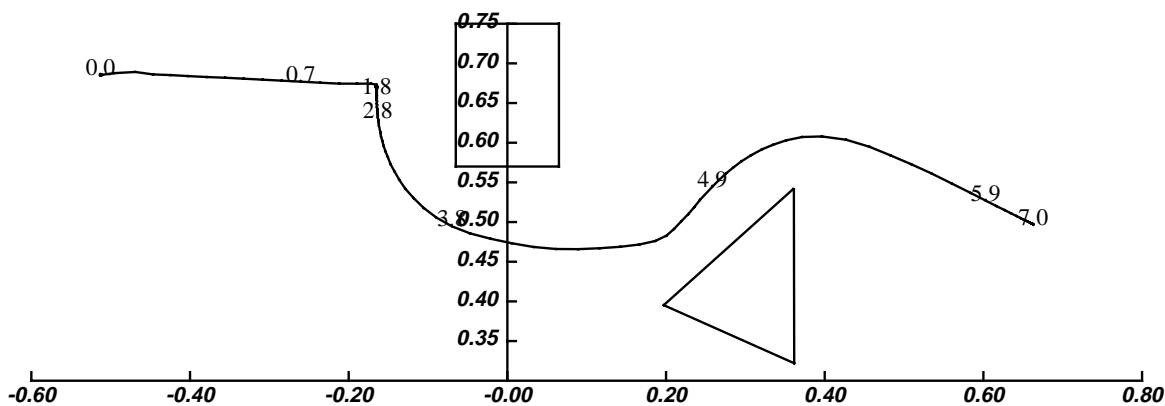


Figure 23: Experimental data showing a path taken to successfully navigate between two objects in a conical well. The well parameters are: $k = 50$ N/m, $s = 0.1$ m, damping = 25 N · s/m. For the rectangle, the potential parameters are: $\alpha = 6$, $A = 0.1$. For the triangle, the potential parameters are: $\alpha = 3$, $A = 0.01$. The numbers along the paths indicate the time in seconds.

tials have been successfully implemented in real time on the CMU DDARM II. The results indicate an improvement over other local potential schemes.

8 Acknowledgements

This research is supported in part by, an AFOSR graduate fellowship (for Richard Volpe), by DARPA under contract DAAA-21-89C-0001, and the Department of Electrical and Computer Engineering.

References

- [1] J. R. Andrews and N. Hogan. Impedance control as a framework for implementing obstacle avoidance in a manipulator. In David E. Hardt and Wayne J. Book, editors, *Control Of Manufacturing Processes And Robotic Systems*, pages 243–251. ASME, 1983.
- [2] R. Bajcsy and F. Solina. Three dimensional object representation revisited. In *First International Conference on Computer Vision*, pages 231–240, London, England, June 8-11 1987.
- [3] A.H. Barr. Superquadrics and angle-preserving transformations. *IEEE Computer Graphics and Applications*, 1:11–23, 1981.
- [4] M. Brady and others (editors). *Robot Motion: Planning and Control*. MIT Press, Cambridge, MA, 1982.
- [5] B. Cohen-Tannoudji, C. Diu, and F. Laloe. *Quantum Mechanics*, volume 2. John Wiley and Sons, New York, 1977.
- [6] B. Faverjon. Obstacle avoidance using an octree in the configuration space of a manipulator. In *Proceedings of the IEEE Conference on Robotics and Automation*, pages 504–512, Atlanta, GA, 1984.
- [7] M. Gardiner. The superellipse: A curve that lies between the ellipse and the rectangle. *Scientific American*, September 1965.
- [8] H. Hanafusa and H. Asada. Stable prehension by a robot hand with elastic fingers. In M. Brady et al., editors, *Robot Motion: Planning and Control*, pages 323–335. MIT Press, 1982.
- [9] N. Hogan. Impedance control: An approach to manipulation. *Journal of Dynamic Systems, Measurement, and Control*, 107:1–24, March 1985.
- [10] O. Khatib. Real-Time Obstacle Avoidance for Manipulators and Mobile Robots. *The International Journal of Robotics Research*, 5(1), 1986.
- [11] P. Khosla and R. Volpe. Superquadric Artificial Potentials for Obstacle Avoidance and Approach. In *Proceedings of the 1988 IEEE International Conference on Robotics and Automation*, Philadelphia, PA, April 26-28, 1988.

- [12] Daniel E. Koditschek. Exact robot navigation by means of potential functions: Some topological considerations. In *IEEE International Conference on Robotics and Automation*, Raleigh, North Carolina, March 31 – April 3 1987.
- [13] B. Krogh. A generalized potential field approach to obstacle avoidance control. In *SME Conf. Proc. Robotics Research: The Next Five Years and Beyond*, Bethlehem, Pennsylvania, August 1984.
- [14] T. Lozano-Perez. Spatial planning: A configuration space approach. *IEEE Transactions on Computers*, C-32(2):102–120, 1983.
- [15] T. Lozano-Perez. A simple motion planning algorithm for general manipulators. Ai lab memo, MIT, AI Labs, Cambridge, MA, 1986.
- [16] T. Lozano-Perez and M. Wesley. An algorithm for planning collision free paths among polyhedral objects. *Comm. of ACM*, 22(10):560–570, 1979.
- [17] J. Luh, M. Walker, and R. Paul. Resolved-acceleration control of mechanical manipulators. *IEEE Transactions on Automatic Control*, 25(3):468–474, June 1980.
- [18] V. Lumelsky and K. Sun. Gross motion planning for a simple 3d articulated robot arm moving amidst unknown arbitrarily shaped objects. In *Proceedings of the IEEE International Conference on Robotics and Automation*, pages 1929–1934, Raleigh, North Carolina, March 31 – April 3 1987.
- [19] W. Newman. Automatic obstacle avoidance at high speeds via reflex control. In *Proceedings of the IEEE Conference on Robotics and Automation*, pages 1104–1109, 1989.
- [20] W. S. Newman and N. Hogan. High speed control and obstacle avoidance using dynamic potential functions. In *IEEE International Conference on Robotics and Automation*, Raleigh, North Carolina, March 31 – April 3 1987.
- [21] M. Okutomi and M. Mori. Decision of robot movement by means of a potential field. *Advanced Robotics*, 1(2):131–141, 1986.
- [22] E. Rimon and E. Koditschek. The construction of analytic diffeomorphisms for exact robot navigation on star worlds. In *Proceedings of the IEEE Conference on Robotics and Automation*, pages 21–26, 1989.
- [23] D. Schmitz, P. Khosla, R. Hoffman, and T. Kanade. Chimera: A real-time programming environment for manipulator control. In *Proceedings of the 27th IEEE International Conference on Robotics and Automation*, Scottsdale, Arizona, May 14-19 1989.
- [24] J. Schwartz and M. Sharir. On the piano movers problem, part ii. Technical Report 41, Courant Institute of Mathematical Sciences, NY, NY, 1982.
- [25] D. Stewart, D. Schmitz, and P. Khosla. Chimera ii: A real-time multiprocessing environment for sensor-based robot control. In *Proceedings of IEEE Int'l Symposium on Intelligent Control*, pages 93–100, Albany, NY, September 1989.

- [26] S. Udupa. Collision detection and avoidance in computer controlled manipulators. In *Proceedings of the 5-th Joint International Conference on AI*. AI, 1977.
- [27] R. Volpe and P. Khosla. Artificial Potentials with Elliptical Isopotential Contours for Obstacle Avoidance. In *Proceedings of the 26th IEEE Conference on Decision and Control*, pages 180–185, Los Angeles, CA, December 9-11, 1987.
- [28] R. Volpe and P. Khosla. A Strategy For Obstacle Avoidance and Approach Using Superquadric Potential Functions. In *Proceedings of the 5th International Symposium of Robotics Research*, pages 93–100, Tokyo, Japan, August 28-31 1989. MIT Press.
- [29] C. Warren. Global path planning using artificial potential fields. In *Proceedings of the IEEE Conference on Robotics and Automation*, pages 316–321, 1989.

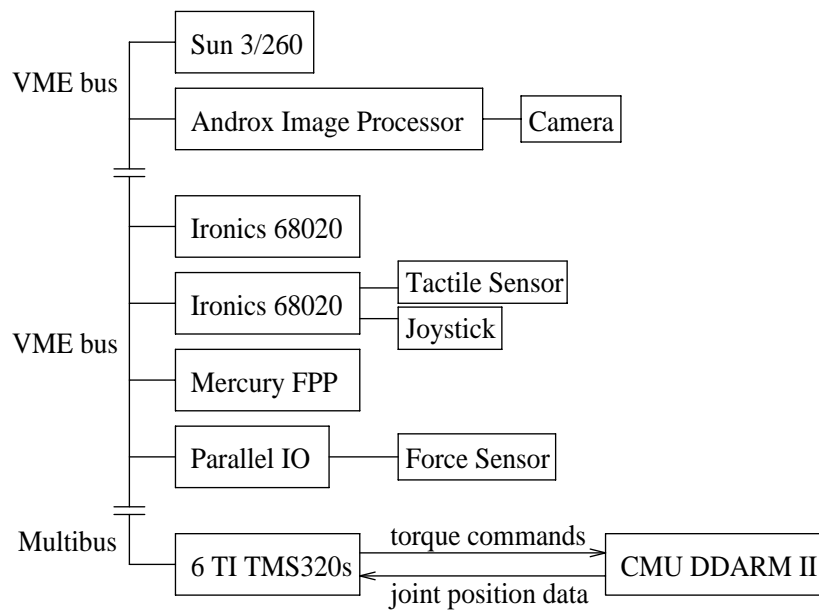


Figure 24: CMU DDARM II control architecture.